



OPEN

Identification of CXCL16 as a diagnostic biomarker for obesity and intervertebral disc degeneration based on machine learning

Jiahao Liu^{1,2}, Jian Zhang^{1,2}, Xiaokun Zhao^{1,2}, Chongzhi Pan^{1,2}, Yuchi Liu^{1,2}, Shengzhong Luo^{1,2}, Xinxin Miao^{1,2,3}, Tianlong Wu^{1,2,3} & Xigao Cheng^{1,2,3}✉

Intervertebral disc degeneration (IDD) is the primary cause of neck and back pain. Obesity has been established as a significant risk factor for IDD. The objective of this study was to explore the molecular mechanisms affecting obesity and IDD by identifying the overlapping crosstalk genes associated with both conditions. The identification of specific diagnostic biomarkers for obesity and IDD would have crucial clinical implications. We obtained gene expression profiles of GSE70362 and GSE152991 from the Gene Expression Omnibus, followed by their analysis using two machine learning algorithms, least absolute shrinkage and selection operator and support vector machine-recursive feature elimination, which enabled the identification of C-X-C motif chemokine ligand 16 (CXCL16) as a shared diagnostic biomarker for obesity and IDD. Additionally, gene set variant analysis was used to explore the potential mechanism of CXCL16 in these diseases, and CXCL16 was found to affect IDD through its effect on fatty acid metabolism. Furthermore, correlation analysis between CXCL16 and immune cells demonstrated that CXCL16 negatively regulated T helper 17 cells to promote IDD. Finally, independent external datasets (GSE124272 and GSE59034) were used to verify the diagnostic efficacy of CXCL16. In conclusion, a common diagnostic biomarker for obesity and IDD, CXCL16, was identified using a machine learning algorithm. This study provides a new perspective for exploring the possible mechanisms by which obesity impacts the development of IDD.

Abbreviations

IDD	Intervertebral disc degeneration
BMI	Body mass index
LASSO	Least absolute shrinkage and selection operator
SVM-RFE	Support vector machine-recursive feature elimination
DEGs	Differentially expressed genes
GEO	Gene Expression Omnibus
WGCNA	Weighted gene coexpression network analysis
ROC	Receiver operating characteristic
GSVA	Gene set variation analysis
ssGSEA	Single-sample gene set enrichment analysis
CXCL16	C-X-C motif chemokine ligand 16
MDSC	Myeloid-derived suppressor cells
TH17 cells	T helper 17 cells

Intervertebral disc degeneration (IDD) constitutes a significant aetiology of lumbar and cervical spinal discomfort¹. The occurrence of IDD leads to a series of diseases in the spine, resulting in a significant burden on the global

¹Department of Orthopedics, The Second Affiliated Hospital of Nanchang University, Nanchang 330006, Jiangxi, China. ²Institute of Orthopedics of Jiangxi Province, Nanchang 330006, Jiangxi, China. ³Institute of Minimally Invasive Orthopedics, Nanchang University, Nanchang 330006, Jiangxi, China. ✉email: xigaocheng@hotmail.com

health care system^{2,3}. The predominant surgical techniques currently employed involve excision of symptomatic intervertebral discs, which can result in compromised functionality, immobilization, and potential complications arising from altered biomechanics⁴. The pathogenesis of IDD remains unclear at present⁵. Considering the complexity of and variability in the factors leading to IDD, it is imperative to identify various triggers and discover distinct diagnostic biomarkers that are aetiology-specific. Such biomarkers could facilitate more precise prevention and treatment of the populations afflicted with IDD.

The risk of IDD is determined by a multitude of factors, as revealed by previous studies^{6–8}. It has been postulated that there may exist a potential risk factor linking IDD to obesity^{9,10}. An upwards trend has been noticed in the incidence of obesity-related low back pain and IDD¹¹. A recent review also pointed out that obesity plays an important role in all diseases that may lead to the occurrence and persistence of low back pain in children¹². Furthermore, it is important to note that in adolescent patients, a significant association has been observed between body mass index (BMI) and IDD, with overweight and obese patients demonstrating greater severity of IDD compared to normal-weight patients¹³. Additionally, according to a comprehensive meta-analysis, one of the primary risk factors for IDD is obesity¹⁴. Moreover, it has been reported that IDD may be influenced by obesity through direct biochemical effects of fatty acids on intervertebral disc cell metabolism¹⁵. The healing process may be impaired due to the nutritional interference of intervertebral discs caused by obesity¹⁶. Additionally, functional leptin receptor expression in intervertebral disc tissue suggests the potential regulation of cell functions by leptin¹⁷. The possible biochemical connection between IDD and obesity is supported by these collective findings. However, common diagnostic biomarkers for IDD and obesity have yet to be reported. Identifying common diagnostic biomarkers for obesity and IDD would greatly aid in the prevention and treatment of IDD in obese patients, thus representing considerable clinical value.

The challenge of biomarker discovery lies in achieving effective feature selection, a fundamental task in this field^{18,19}. To address this issue, a combination of several machine learning approaches can be utilized²⁰. In recent years, the application of advanced machine learning algorithms has become prevalent in the screening of medical biomarkers^{21,22}. The least absolute shrinkage and selection operator (LASSO), which combines feature selection and regularization, is a machine learning technique that can construct a penalty function to address complex collinearity data and produce an improved linear model. The refined linear model generated by the lasso algorithm is an effective approach to solving this problem²³. Similarly, the extensively utilized machine learning technique support vector machine-recursive feature elimination (SVM-RFE) finds wide application in various biological fields characterized by a feature size that surpasses the available number of samples, as observed in metabolomic analyses²⁴. The aim of this study was to screen for shared diagnostic biomarkers associated with obesity and IDD using two machine algorithms, LASSO and SVM-RFE, with the ultimate goal of identifying potential therapeutic and diagnostic targets for the management and prevention of obesity-related IDD.

Materials and methods

Dataset download and data preprocessing

The raw gene expression profile data were obtained from the Gene Expression Omnibus (GEO) by conducting a search for RNA-seq profiles using relevant keywords such as "obesity" and "intervertebral disc degeneration". Two training datasets (GSE70362 and GSE152991) and two validation datasets (GSE124272 and GSE59034) were identified. GSE70362 comprised 16 IDD subjects and 8 normal controls, while GSE152991 included 34 obese patients and 11 normal controls. The validation datasets consisted of GSE124272 (8 IDD patients and 8 controls) and GSE59034 (16 obese patients and 16 normal controls). The data were subjected to background correction and normalization using the R package "limma".

Identification of differentially expressed genes (DEGs)

The identification of DEGs between samples from healthy controls and patients was conducted utilizing the R package "limma" with a screening criterion consisting of a Wilcoxon test and a *p* value threshold of less than 0.05.

Construction and module analysis via weighted gene coexpression network analysis (WGCNA)

The WGCNA software package R.4.2.3, which employs weighted gene coexpression network analysis, was utilized to conduct coexpression network construction and correlation analysis between clinical features regarding obesity and IDD. Key modules associated with the diseases were identified based on the eigengenes' Pearson correlation coefficient and *P* value.

GO and KEGG enrichment analysis of shared genes

Correlation analysis among DEGs was performed using the R package "corrplot". To explore comprehensive information on large-scale gene data, GO enrichment analysis and KEGG pathway enrichment analysis²⁵ (<https://www.kegg.jp>) were employed as common bioinformatic methods. The results of these analyses were visualized using the "GOplot" program package. In addition, Metascape (<http://metascape.org>), an online analytical tool, was utilized to analyse possible diseases (DisGeNET database) related to shared genes.

Screening diagnostic biomarkers via machine learning algorithms

Diagnostic biomarkers for obesity and IDD were screened using two machine learning algorithms: LASSO and SVM-RFE. The R packages "glmnet" and "e1071" were utilized to perform LASSO regression and SVM-RFE. A shared diagnostic biomarker for the two aforementioned diseases was obtained by employing a Venn plot.

Development and verification of a diagnostic biomarker

The significance of the difference in diagnostic biomarkers between the disease and control groups was evaluated using a significance threshold of $p < 0.05$, with subsequent assessment of the potential diagnostic biomarker's predictive ability in the validation dataset carried out through receiver operating characteristic (ROC) analysis utilizing the "pROC" package.

Gene set variation analysis (GSVA) of the diagnostic biomarker

To investigate the potential biological functions of the diagnostic biomarker, GSVA was conducted using the R package "clusterprofiler" based on GO and KEGG gene sets. The reference gene sets `c5.go.Symbols.gmt` and `c2.cp.kegg.Symbols.gmt` were employed. Enriched functional categories and pathways were identified by applying a cut-off criterion of a p-adjusted value of < 0.05 .

Evaluation and correlation analysis of immune infiltrating cells

The extent of immune cell infiltration and the nature of infiltrating immune cells were explored through single-sample gene set enrichment analysis (ssGSEA) of 28 immune-related signatures derived from expression profiles to reveal differences in the correlations between the diagnostic biomarker and immune infiltrating cells. Using "gsva" function for ssGSEA. Furthermore, the "ggplot2" package was employed to visualize the results.

Statistical analysis

All data processing and analysis were performed using R software (version 4.2.3). Differences between independent and non-normally distributed variables were analyzed using the Wilcoxon test. Spearman correlation analysis was conducted to calculate the correlation coefficients between different genes, the correlation between genes and immune cells, as well as the module-trait associations. $P < 0.05$ was considered statistically significant.

Results

Identification of shared genes in IDD and obesity

To clearly demonstrate the specific process of this study, the bioinformatics analysis process is summarized in Fig. 1. A total of 3102 upregulated and 3744 downregulated DEGs were detected between obese patients and normal controls (Fig. 2A). In obesity, the relationships between modules were evaluated by drawing a heatmap based on the Spearman correlation coefficient for the module-trait associations (Fig. 2B). Three modules for obesity were identified by WGCNA, and the blue module was clinically most significant and was chosen as an obesity-related module ($r = -0.82$, $p = 7e-12$, genes = 140) (Fig. 2C). Additionally, a total of 1741 DEGs were identified between IDD patients and normal controls, of which 802 DEGs were upregulated and 939 DEGs were downregulated, as revealed in the heatmaps (Fig. 2D). In IDD, the relationships between modules were evaluated by drawing a heatmap based on the Spearman correlation coefficient for the module-trait associations (Fig. 2E). Five modules for IDD were identified by WGCNA, and the ME in the blue module was clinically more significant for IDD than any other module, which was chosen as the IDD-related module ($r = -0.63$, $p = 9e-04$, genes = 13) (Fig. 2F). By intersecting genes in DEGs and the most positive modules, a total of 15 shared genes were obtained, which may be associated with the pathogenesis of obesity and IDD (Fig. 2G).

Enrichment of functions and pathways of shared genes

A strong and significant correlation was observed between most shared genes in the obesity samples (Fig. 3A), as was the case in the IDD samples (Fig. 3B). The GO analysis showed that shared genes were mainly enriched in the regulation of osteoclast differentiation, leukocytes and chemotaxis (Fig. 3C). Additionally, KEGG analysis revealed a significant enrichment in shared genes in the chemokine signalling pathway, cytokine–cytokine receptor interaction, and carbohydrate digestion and absorption (Fig. 3D). The enrichment analysis in DisGeNET showed that shared genes were associated with inflammation and myalgia (Fig. 3E).

Identification of potential shared diagnostic markers

LASSO and SVM-RFE are both machine learning methods for screening characteristic genes. Based on the 15 shared genes, 5 possible diagnostic biomarkers for obesity were identified by LASSO (Fig. 4A), and 2 possible diagnostic biomarkers for obesity were identified by SVM-RFE (Fig. 4B, C). Additionally, 9 possible diagnostic biomarkers for IDD were identified by LASSO (Fig. 4D), and 9 possible diagnostic biomarkers for IDD were identified by SVM-RFE (Fig. 4E, F). Ultimately, we determined that C-X-C motif chemokine ligand 16 (CXCL16) was the best diagnostic biomarker for the development of IDD and obesity by Venn analysis (Fig. 4G).

Differential expression analysis and ROC curve of CXCL16 in obesity and IDD

We found that CXCL16 was significantly differentially expressed between the disease group and the control group and had good diagnostic efficacy according to the ROC curve. Differential expression analysis showed that CXCL16 was significantly overexpressed in obesity (Fig. 5A) and significantly underexpressed in IDD (Fig. 5C). By ROC curve analysis, we obtained an AUC of 0.981 for obesity (Fig. 5B), and the results showed that the AUC was 0.766 for IDD (Fig. 5D). The same results for CXCL16 were verified in an independent obesity validation dataset, GSE59034 (Fig. 5E), and an independent IDD validation dataset, GSE124272 (Fig. 5G). The ROC curve showed an AUC = 0.930 in the obesity test cohort (Fig. 5F) and an AUC = 0.781 in the IDD test cohort (Fig. 5H).

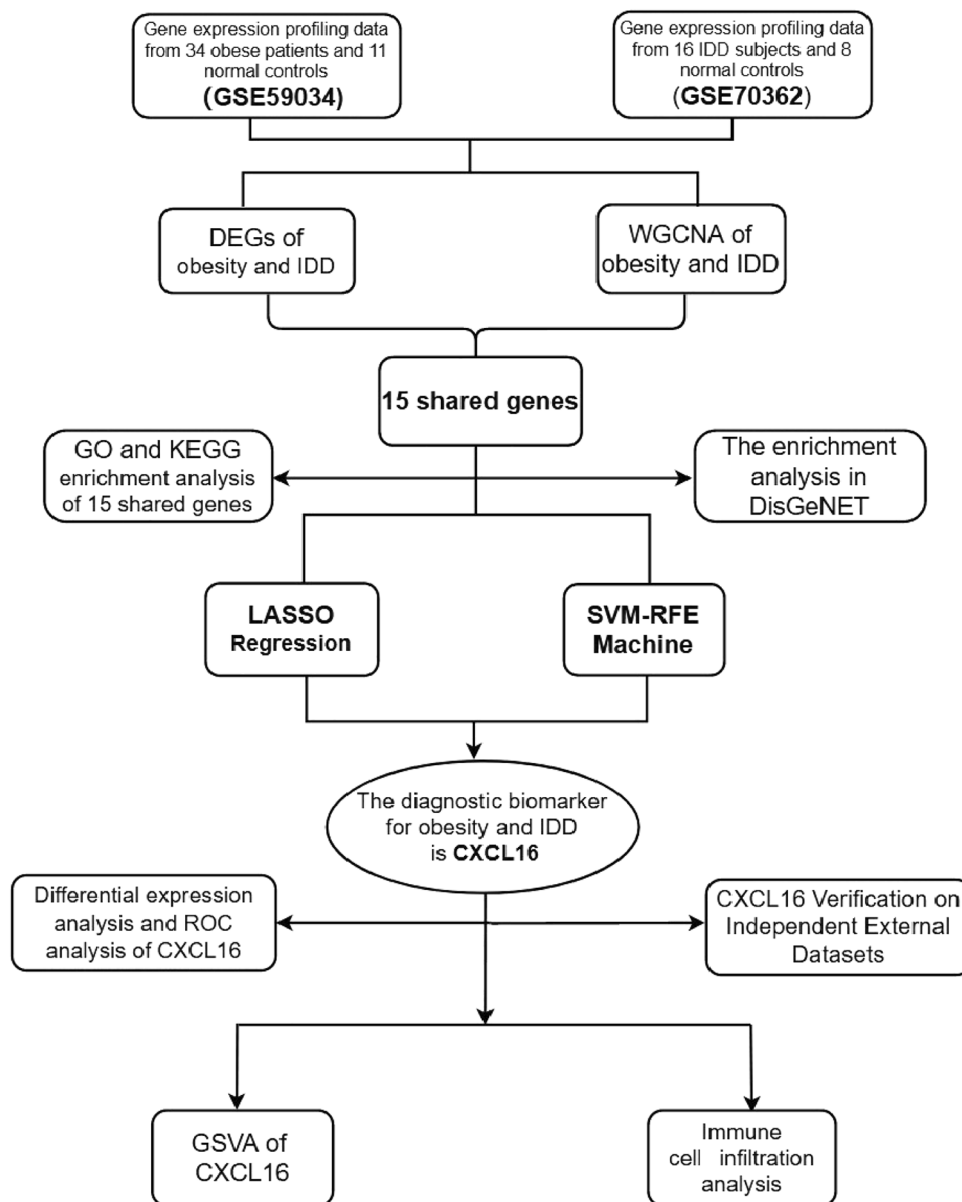


Figure 1. Analysis flow chart.

GSVA enrichment analysis of CXCL16 in IDD and obesity

In obesity, the GO functions of the CXCL16 low-expression group were enriched in the regulation of macrophage fusion and chitin metabolic processes (Fig. 6A). The KEGG pathways of the CXCL16 high-expression group were mainly enriched in linoleic acid metabolism and fatty acid metabolism, and in the CXCL16 low-expression group of obesity, the pathways were mainly enriched in other glycan degradation and toll-like receptor signalling pathways (Fig. 6C). In IDD, GO functions of the CXCL16 high-expression group were enriched in mhc-class-ii-receptor-activity and triple codon amino acid adaptor activity (Fig. 6B). KEGG pathways of the CXCL16 low-expression group were mainly enriched in pantothenate and CoA biosynthesis and glycosaminoglycan, specifically keratan sulfate, biosynthesis (Fig. 6D).

Immune cell infiltration analysis

The effect of immune cells on disease was analysed by comparing differences in immune cell levels between the normal and control groups in the 2 datasets using ssGSEA. In GSE152991, lower levels of central memory CD8 T cells were observed in obesity samples compared to normal controls. Levels of activated B cells, activated CD4 T cells, activated dendritic cells, CD56 bright natural killer cells, CD56dim natural killer cells, gamma delta T cells, immature B cells, myeloid-derived suppressor cells (MDSC), macrophages, mast cells, monocytes, natural killer T cells, natural killer cells, plasmacytoid dendritic cells, regulatory T cells, T-follicular helper cells, type 1 T helper cells, effector memory CD4 T cells and central memory CD4 T cells were higher in obesity samples than

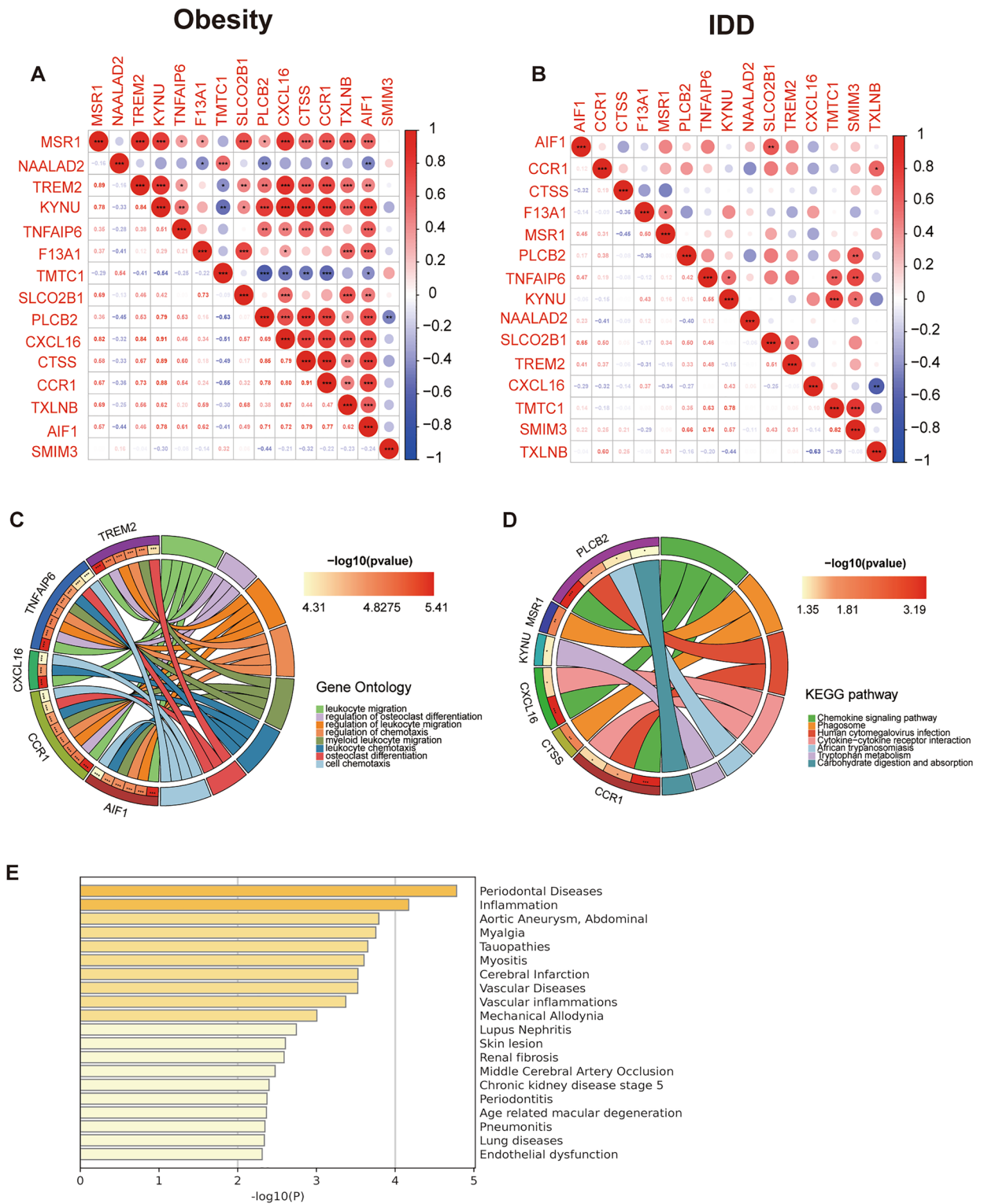


Figure 3. Enrichment analysis of 15 shared genes. (A) Correlation analysis of 15 shared genes for obesity. (B) Correlation analysis of 15 shared genes for IDD. (C) GO analysis of 15 shared genes. (D) KEGG analysis of 15 shared genes for obesity. (E) Summary of enrichment analysis in DisGeNET.

for IDD and obesity, CXCL16, was identified with machine learning algorithms, and the potential mechanism of CXCL16 action was explored by GSEA. Furthermore, we analysed the regulatory effect of CXCL16 on immune cell infiltration, and our findings may provide potential applications for obese and IDD patients, such as early diagnosis, treatment monitoring.

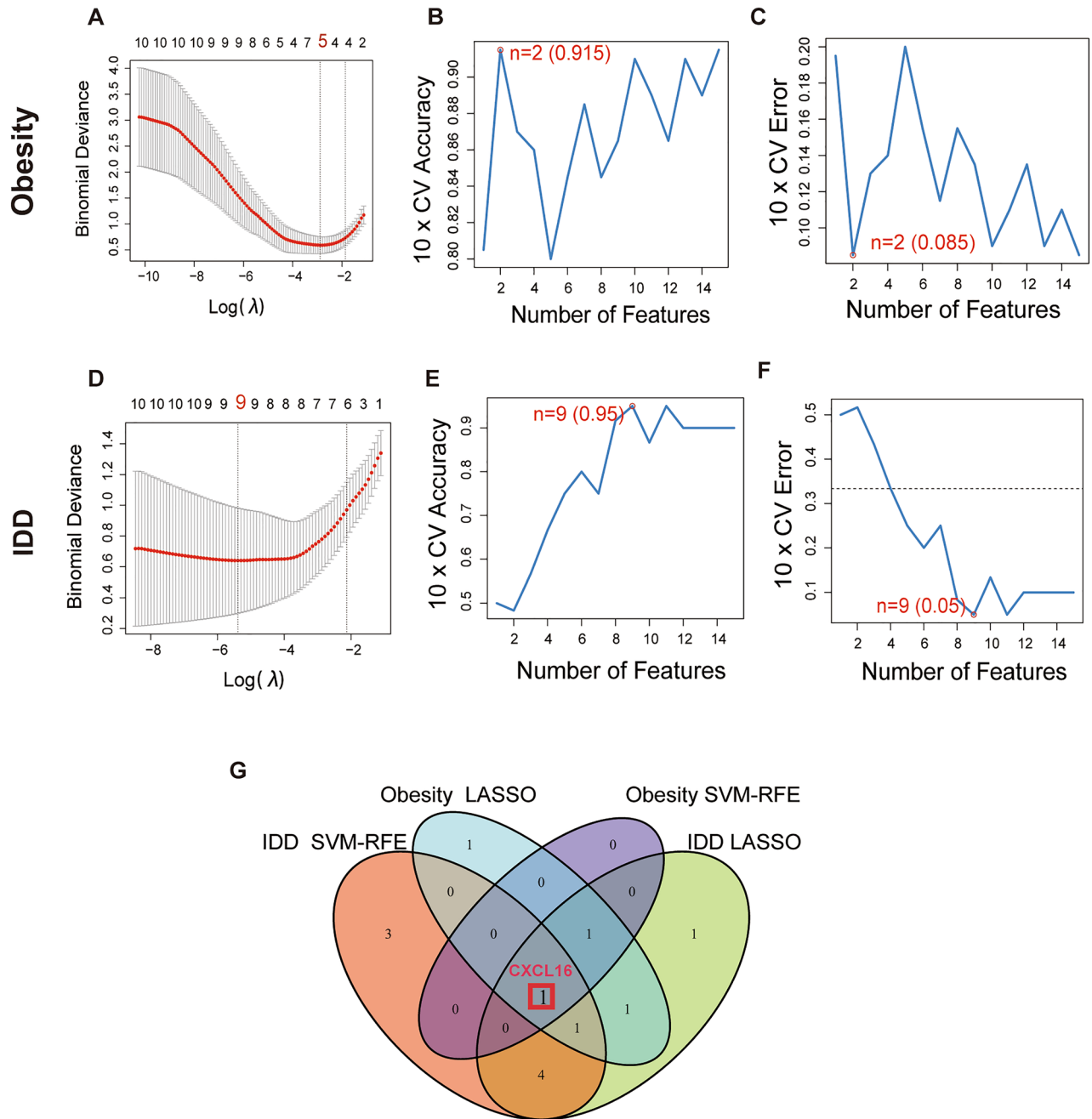


Figure 4. Machine learning to screen diagnostic markers. (A) LASSO to screen diagnostic markers for obesity. (B, C) SVM-RFE to screen diagnostic markers for obesity. (D) LASSO to screen diagnostic markers for IDD. (E, F) SVM-RFE to screen diagnostic markers for IDD. (E) Venn diagram showing a diagnostic gene in IDD and obesity.

The CXC chemokine subfamily encompasses various members, one of which is CXCL16. In contrast to other members of this subgroup, CXCL16 possesses a unique structural composition consisting of four distinct domains. A chemokine domain is present, which is connected to the cell surface through a mucin-like stack, and this stack is further linked to transmembrane and cytoplasmic domains²⁹. It plays a significant role in the progression of cancer^{30–32} as well as the course of atherosclerosis, renal fibrosis, nonalcoholic fatty liver disease (NAFLD) and pulmonary fibrosis^{33–38}. The promotion of disc degeneration by CXCL16 was found to affect fatty acid metabolism, which is consistent with previous research. Previous studies have demonstrated that disk cell metabolism is directly influenced by fatty acids in the context of obesity-mediated apoptosis and extracellular matrix metabolic imbalances via MAPK pathway activation in intervertebral disk degeneration¹⁵. However, previous studies have not identified the specific molecular mechanism by which nucleus pulposus cell apoptosis occurs through the MAPK pathway, and the diagnostic biomarker we have selected this time, CXCL16, is likely to be involved in the MAPK pathway as a potential biomolecule that promotes IDD.

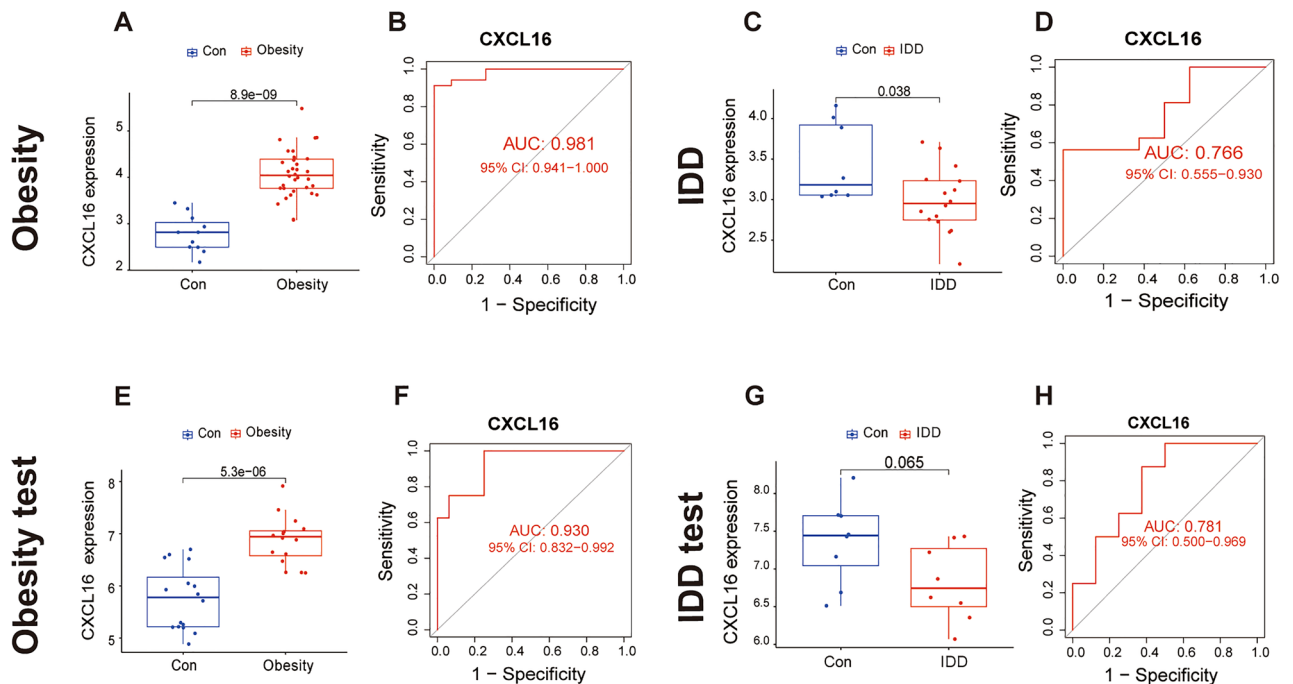


Figure 5. Differential expression analysis and ROC curve of CXCL16. (A) Differential expression of CXCL16 in obesity. (B) ROC curve evaluating the CXCL16 diagnostic efficacy in obesity. (C) Differential expression of CXCL16 in IDD. (D) ROC curve evaluating the CXCL16 diagnostic efficacy in IDD. (E) Differential expression of CXCL16 in the obesity test cohort. (F) ROC curve evaluating the CXCL16 diagnostic efficacy in the obesity test cohort. (G) Differential expression of CXCL16 in the IDD test cohort. (H) ROC curve evaluating the CXCL16 diagnostic efficacy in the IDD test cohort.

By analysing the correlation between CXCL16 and immune cells, we found that CXCL16 negatively regulates T helper 17 cells (TH17 cells). Interleukin 17-producing TH17 cells, which belong to a subtype of helper T cells, are recognized as crucial drivers in the development of both autoimmunity and inflammation³⁹. TH17 cells of human origin are frequently observed in peripheral tissues and organs^{40,41}. Numerous human diseases may be influenced by TH17-cell activity and should not be overlooked^{42–44}. During an inflammatory response, the primary role of TH17 cells is to facilitate the recruitment of inflammatory immune cells to infected or damaged tissue. This can result in the exacerbation of autoimmune diseases and chronic inflammatory conditions⁴⁵. On the basis of our analysis, we found that in IDD, CXCL16 expression was low, which promoted the infiltration of TH17 cells in the intervertebral disc, which may exacerbate the inflammatory response of the intervertebral disc and thus promote degeneration of the intervertebral disc.

Although diagnostic biomarkers associated with obesity and IDD have been identified by machine learning algorithms, their diagnostic efficiency has been confirmed in external datasets. However, this study only showed the correlation of CXCL16 in the effects of IDD and obesity, and whether CXCL16 mediates the development of IDD in obese patients needs to be further investigated. In addition, our study is limited to basic sample characteristics and expression data obtained from GEO database. We were unable to access more detailed clinical information, such as age, complications, BMI, degree of IDD by the Pfirrmann grade, involved disc levels, and type of IDD (e.g., disc herniation, spinal stenosis, degenerative spondylolisthesis, disc disease), which restricts our ability to rule out other confounding factors that may affect the expression of CXCL16 and other inflammatory marker genes. This limitation in our study can potentially influence the interpretation of the identified common diagnostic markers from both IDD and obesity-related gene expression datasets. In future studies, we will validate our conclusions by designing prospective cohort studies to collect more comprehensive and multidimensional data. Moreover further experimental validation is needed to comprehensively understand the role of this diagnostic marker and its potential regulatory mechanisms related to IDD and obesity by techniques such as RT-qPCR and Western blotting.

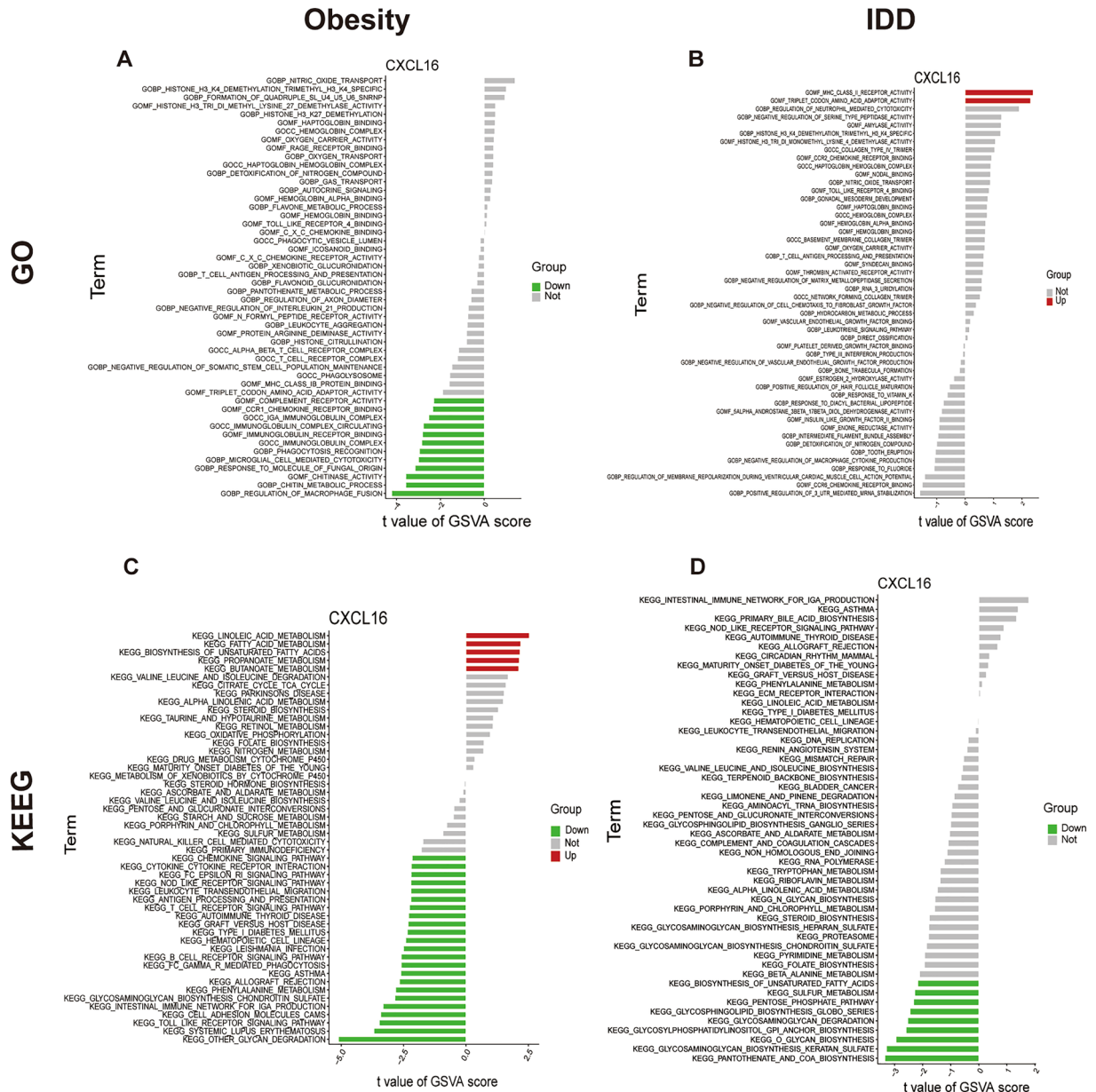


Figure 6. GSA of CXCL16. (A) GO analysis based on GSA of CXCL16 in obesity. (B) GO analysis based on GSA of CXCL16 in IDD. (C) KEGG analysis based on GSA of CXCL16 in obesity. (D) KEGG analysis based on GSA of CXCL16 in IDD.

Conclusions

We identified CXCL16 as a diagnostic biomarker for obesity and IDD in this study by machine learning methods. CXCL16 was investigated by GSA to promote disc degeneration in IDD mainly by affecting fatty acid metabolism, as demonstrated by diagnostic biomarker and immune cell correlation analysis, revealing that CXCL16 promotes disc degeneration by regulating T helper 17 cell infiltration. Our analysis provides a new perspective for further exploring the underlying mechanisms by which obesity impacts IDD, and we will subsequently perform relevant *in vitro* and *in vivo* experiments.

8. Battié, M. C. *et al.* 1991 Volvo Award in clinical sciences. Smoking and lumbar intervertebral disc degeneration: an MRI study of identical twins. *Spine (Phila Pa 1976)* **16**, 1015–1021 (1991).
9. Heliövaara, M. Body height, obesity, and risk of herniated lumbar intervertebral disc. *Spine (Phila Pa 1976)* **12**, 469–472 (1987).
10. Liuke, M. *et al.* Disc degeneration of the lumbar spine in relation to overweight. *Int J Obes (Lond)* **29**, 903–908 (2005).
11. Ranson, W. A. *et al.* Risk Factors for Perioperative Complications in Morbidly Obese Patients Undergoing Elective Posterior Lumbar Fusion. *Global Spine J* **8**, 795–802 (2018).
12. Ambrosio, L. *et al.* The burden of low back pain in children and adolescents with overweight and obesity: from pathophysiology to prevention and treatment strategies. *Ther Adv Musculoskelet Dis* **15**, 1759720X231188831 (2023).
13. Samartzis, D. *et al.* A population-based study of juvenile disc degeneration and its association with overweight and obesity, low back pain, and diminished functional status. *J Bone Joint Surg Am* **93**, 662–670 (2011).
14. Xu, X., Li, X. & Wu, W. Association Between Overweight or Obesity and Lumbar Disk Diseases: A Meta-Analysis. *J Spinal Disord Tech* **28**, 370–376 (2015).
15. Zhang, X. *et al.* Obesity Mediates Apoptosis and Extracellular Matrix Metabolic Imbalances via MAPK Pathway Activation in Intervertebral Disk Degeneration. *Front Physiol* **10**, 1284 (2019).
16. Shiri, R., Lallukka, T., Karppinen, J. & Viikari-Juntura, E. Obesity as a risk factor for sciatica: a meta-analysis. *Am J Epidemiol* **179**, 929–937 (2014).
17. Zhao, C.-Q., Liu, D., Li, H., Jiang, L.-S. & Dai, L.-Y. Expression of leptin and its functional receptor on disc cells: contribution to cell proliferation. *Spine (Phila Pa 1976)* **33**, E858–864 (2008).
18. Baumgartner, C., Osl, M., Netzer, M. & Baumgartner, D. Bioinformatic-driven search for metabolic biomarkers in disease. *J Clin Bioinforma* **1**, 2 (2011).
19. Saeys, Y., Inza, I. & Larrañaga, P. A review of feature selection techniques in bioinformatics. *Bioinformatics* **23**, 2507–2517 (2007).
20. Grissa, D. *et al.* Feature Selection Methods for Early Predictive Biomarker Discovery Using Untargeted Metabolomic Data. *Front Mol Biosci* **3**, 30 (2016).
21. Huang, L. *et al.* Machine learning of serum metabolic patterns encodes early-stage lung adenocarcinoma. *Nat Commun* **11**, 3556 (2020).
22. Shen, B. *et al.* Proteomic and Metabolomic Characterization of COVID-19 Patient Sera. *Cell* **182**, 59–72.e15 (2020).
23. Zhang, P. *et al.* Machine learning applied to serum and cerebrospinal fluid metabolomes revealed altered arginine metabolism in neonatal sepsis with meningoencephalitis. *Comput Struct Biotechnol J* **19**, 3284–3292 (2021).
24. Gromski, P. S. *et al.* A comparative investigation of modern feature selection and classification approaches for the analysis of mass spectrometry data. *Anal Chim Acta* **829**, 1–8 (2014).
25. Ogata, H. *et al.* KEGG: Kyoto Encyclopedia of Genes and Genomes. *Nucleic Acids Res* **27**, 29–34 (1999).
26. Li, Z. *et al.* The role of leptin on the organization and expression of cytoskeleton elements in nucleus pulposus cells. *J Orthop Res* **31**, 847–857 (2013).
27. Hu, S. *et al.* Chemerin facilitates intervertebral disc degeneration via TLR4 and CMKLR1 and activation of NF- κ B signaling pathway. *Aging (Albany NY)* **12**, 11732–11753 (2020).
28. Battié, M. C., Videman, T., Levälahti, E., Gill, K. & Kaprio, J. Genetic and environmental effects on disc degeneration by phenotype and spinal level: a multivariate twin study. *Spine (Phila Pa 1976)* **33**, 2801–2808 (2008).
29. Matloubian, M., David, A., Engel, S., Ryan, J. E. & Cyster, J. G. A transmembrane CXC chemokine is a ligand for HIV-coreceptor Bonzo. *Nat Immunol* **1**, 298–304 (2000).
30. Zhu, Y. *et al.* MEK inhibitor diminishes nasopharyngeal carcinoma (NPC) cell growth and NPC-induced osteoclastogenesis via modulating CCL2 and CXCL16 expressions. *Tumour Biol* **36**, 8811–8818 (2015).
31. Hald, S. M. *et al.* Prognostic impact of CXCL16 and CXCR6 in non-small cell lung cancer: combined high CXCL16 expression in tumor stroma and cancer cells yields improved survival. *BMC Cancer* **15**, 441 (2015).
32. Hu, W., Liu, Y., Zhou, W., Si, L. & Ren, L. CXCL16 and CXCR6 are coexpressed in human lung cancer in vivo and mediate the invasion of lung cancer cell lines in vitro. *PLoS One* **9**, e99056 (2014).
33. Ma, Z. *et al.* CXCL16/CXCR6 axis promotes bleomycin-induced fibrotic process in MRC-5 cells via the PI3K/AKT/FOXO3a pathway. *Int Immunopharmacol* **81**, 106035 (2020).
34. Jiang, L. *et al.* CXC Motif Ligand 16 Promotes Nonalcoholic Fatty Liver Disease Progression via Hepatocyte-Stellate Cell Crosstalk. *J Clin Endocrinol Metab* **103**, 3974–3985 (2018).
35. Xia, Y., Yan, J., Jin, X., Entman, M. L. & Wang, Y. The chemokine receptor CXCR6 contributes to recruitment of bone marrow-derived fibroblast precursors in renal fibrosis. *Kidney Int* **86**, 327–337 (2014).
36. Aslanian, A. M. & Charo, I. F. Targeted disruption of the scavenger receptor and chemokine CXCL16 accelerates atherosclerosis. *Circulation* **114**, 583–590 (2006).
37. Xu, H. *et al.* Involvement of up-regulated CXC chemokine ligand 16/scavenger receptor that binds phosphatidylserine and oxidized lipoprotein in endotoxin-induced lethal liver injury via regulation of T-cell recruitment and adhesion. *Infect Immun* **73**, 4007–4016 (2005).
38. Minami, M. *et al.* Expression of scavenger receptor for phosphatidylserine and oxidized lipoprotein (SR-PSOX) in human atheroma. *Ann N Y Acad Sci* **947**, 373–376 (2001).
39. Hirschfeld, G. M. & Siminovitch, K. A. Toward the molecular dissection of primary biliary cirrhosis. *Hepatology* **50**, 1347–1350 (2009).
40. Zou, W. & Restifo, N. P. TH17 cells in tumour immunity and immunotherapy. *Nat Rev Immunol* **10**, 248–256 (2010).
41. Kryczek, I. *et al.* Phenotype, distribution, generation, and functional and clinical relevance of Th17 cells in the human tumor environments. *Blood* **114**, 1141–1149 (2009).
42. Martin-Orozco, N. *et al.* T helper 17 cells promote cytotoxic T cell activation in tumor immunity. *Immunity* **31**, 787–798 (2009).
43. Kleinschek, M. A. *et al.* Circulating and gut-resident human Th17 cells express CD161 and promote intestinal inflammation. *J Exp Med* **206**, 525–534 (2009).
44. Kryczek, I. *et al.* Induction of IL-17+ T cell trafficking and development by IFN- γ : mechanism and pathological relevance in psoriasis. *J Immunol* **181**, 4733–4741 (2008).
45. Lee, Y. *et al.* Induction and molecular signature of pathogenic TH17 cells. *Nat Immunol* **13**, 991–999 (2012).

Acknowledgements

The data provided by participants in GEO, including patients and researchers, is sincerely appreciated by the authors.

Author contributions

J.L.: Methodology, Visualization, Writing—Original Draft, Writing—review & editing. J.Z. and X.Z.: Methodology, Investigation, Writing—Original Draft. C.P., Y.L. and S.L.: Writing—Review and Editing. X.M. and T.W.: Writing—review and editing. X.C.: conceptualization, supervision. All authors have read and agreed to the published version of the manuscript. All authors reviewed and approved the final version of the manuscript.

Funding

The present study was supported by the National Natural Science Foundation of China (grant no. 82060403) and the Thousand Talents Program of Jiangxi Province, China (grant no. JXSQ2019201026).

Competing interests

The authors declare no competing interests.

Additional information

Correspondence and requests for materials should be addressed to X.C.

Reprints and permissions information is available at www.nature.com/reprints.

Publisher's note Springer Nature remains neutral with regard to jurisdictional claims in published maps and institutional affiliations.



Open Access This article is licensed under a Creative Commons Attribution 4.0 International License, which permits use, sharing, adaptation, distribution and reproduction in any medium or format, as long as you give appropriate credit to the original author(s) and the source, provide a link to the Creative Commons licence, and indicate if changes were made. The images or other third party material in this article are included in the article's Creative Commons licence, unless indicated otherwise in a credit line to the material. If material is not included in the article's Creative Commons licence and your intended use is not permitted by statutory regulation or exceeds the permitted use, you will need to obtain permission directly from the copyright holder. To view a copy of this licence, visit <http://creativecommons.org/licenses/by/4.0/>.

© The Author(s) 2023